

RESEARCH ARTICLE

Superposition network coded cooperation for wireless networks

Ali Fazeli¹, Mohammad Javad Omid¹, Hamid Saeedi-Sourck^{2*} and Masoud Ardakani³¹ Electrical and Computer Engineering Department, Isfahan University of Technology, Isfahan 84156-83111, Iran² Electrical Engineering Department, Yazd University, Yazd 89158-18411, Iran³ Electrical and Computer Engineering Department, University of Alberta, Edmonton, AB, Canada

ABSTRACT

Cooperative diversity is an innovative approach to improve the reliability of communication. Although this technique is considered in the next-generation mobile communication standards, it has its own challenges in practice. For example, in simultaneous transmission-based cooperative protocols, perfect synchronisation of nodes is very hard to realise. The traditional time division multiple access method can simplify the synchronisation problems but leads to long transmission delays. In this paper, a low-delay cooperative strategy is proposed for a network with multiple sources and a single destination, which requires only a simple type of synchronisation. In this technique, we use a combination of superposition coding and network coding; hence the name superposition network coded cooperation. For this strategy, good bounds are obtained for the probability of correct detection for general M-PSK and M-QAM modulation and are compared with simulation results. The results demonstrate improvement in error performance compared with other transmission schemes requiring the same transmission time as superposition network coded cooperation. Copyright © 2016 John Wiley & Sons, Ltd.

*Correspondence

H. Saeedi-Sourck, Electrical Engineering Department, Yazd University, Yazd 89158-18411, Iran.

E-mail: saeedi@yazd.ac.ir

Received 17 January 2016; Revised 18 March 2016; Accepted 27 March 2016

1. INTRODUCTION

Communication over a wireless channel is subject to large-scale propagation effects including path loss and shadowing, and to small-scale multipath fading. These are some of the most important sources of performance degradation. Various techniques based on time, frequency and spatial diversity have been proposed to mitigate the adverse effects of fading [1]. Exploiting diversity by transmitting over spatially independent channels, called spatial diversity, is of great importance.

Cooperative communication is a practical approach to exploit spatial diversity [2, 3]. This technique has been widely investigated from industrial perspective and is considered as a desirable and promising approach to next generation wireless technologies [4, 5]. The fundamental idea of cooperative communication is to use the cooperation among a group of distributed nodes to form a virtual multiple antenna system [6].

Although cooperative communication is a practical solution to improve the performance of wireless systems, it has its own challenges. Practical networks are composed of many nodes, so efficient cooperative diversity protocols

involve multiple relays. Some multi-relay cooperative protocols have been considered in [7–14]. The performance of multi-relay decode-and-forward and amplify-and-forward protocols using conventional repetition coding was studied in [7–10]. In repetition coding, all relay nodes retransmit the source information on orthogonal channels in a time division multiple access (TDMA) manner to avoid inter-relay interference. Although this is a low-complexity approach, it leads to long time delays. The delay caused by repetition coding is also dependent on the number of relay nodes [6]. Thus, these protocols are not efficient for networks with large numbers of relays. To reduce transmission delays, simultaneous transmission-based protocols have been proposed [11–14], in which more than one node can transmit in one time slot by using frequency division multiple access, code division multiple access or distributed space-time codes. For these cooperative schemes, time and frequency offsets at the receiver cause inter-symbol interference, which degrades communication performance severely. So it is crucial in these techniques to have no time and frequency mismatches. On the other hand, these mismatches are unavoidable because of the distributed nature of cooperative communication. In fact, the different

propagation and processing time among nodes and timing estimation errors are the main reasons of timing offsets at the receiver [15–17]. Furthermore, there is a frequency mismatch between different nodes because of doppler effects and oscillator instabilities. Overall, because of the different sources of time and frequency offsets, it is difficult for the receiver to compensate for all the mismatches. In conclusion, although traditional simultaneous transmission-based cooperative strategies result in significant improvement in transmission delay, they usually require perfect time and frequency synchronisation of the nodes [18].

It can be concluded that new low-delay solutions for cooperation with simple synchronisation requirements are highly desirable. In [17], utilising orthogonal frequency division multiplexing, a new simultaneous transmission-based strategy, is suggested for asynchronous relay networks to improve the communication performance, degraded because of the time synchronisation problem.

In this paper, a new cooperative multi-message multicast scheme for a single destination is proposed. We consider a network, where multiple users transmit their information symbols to the common destination using relay nodes. To have simple synchronisation requirements, simultaneous transmission of nodes is not allowed, and TDMA is used for transmission [18, 19]. Although exact synchronisation for simultaneous transmission-based cooperative schemes is highly challenging, it is not a difficult problem for TDMA-based cooperative strategies. In fact, by transmitting a single signal in each time slot, the time and frequency mismatches at the receiver are easier to determine than those of simultaneous transmission-based schemes and can be corrected by using a simple phased-locked loop device at the receiver [18]. In order to provide the lowest possible time delay, we use a technique called superposition coded cooperation (SCC) [5, 20–25]. The basic idea of SCC is to transmit a signal, made of a suitable combination of multiple signals, to destination [20]. To describe SCC, we assume there are two or more information signals available at a specific transmitter. Each of the signals can belong to the transmitter or to other source nodes. In other words, some of the signals may be from other source nodes, received by the transmitter in previous transmission phases. The transmitter allocates its transmit power to the signals in a defined manner, adds them together and then transmits the resulted composite signal in its transmission phase [5, 20–25]. In [5], for providing higher spatial diversity gain in a network, a cooperative multicast scheme with one source node is proposed, where the source node, using SCC, broadcasts a composite signal, made of two messages, to a group of receivers. To achieve optimal diversity-multiplexing trade-off, a two-way multi-relay cooperative scheme based on superposition coding is proposed in [21]. In this work, the information symbols of two source nodes are combined in a relay node, selected among a group of relays according to some criteria, and then sent to destination nodes. The analysis of achievable rate and expected rate of a cooperative scheme

based on SCC in a three-node relay network with one source node, sending a symbol composed of two messages, is proposed in [22]. In [23], a combination of hierarchical modulation and SCC is used in a network with two source nodes, one relay node and one destination, to improve performance in terms of spectral efficiency, block error rate and capacity. The outage analysis of a SCC scheme in a network composed of multiple source-destination nodes and one relay node is proposed in [24]. In this work, it is assumed that after the source transmission phase, the relay node transmits a composite symbol, containing the symbols it has managed to detect correctly, to all destinations, free from error. A software radio system for superposition coding is designed and implemented in [25] to study the performance of this technique practically. The results has shown remarkable gains in spectral efficiency in comparison with orthogonal schemes such as TDMA. Because of its advantages, superposition coding is considered as promising approach for future technologies including future cellular networks, *ad hoc* networks and software radio technologies [25, 26]. An advantage of SCC, used in this paper, is that the source and the relay transmission phases for a communication node can be performed at the same time, eliminating time delays caused by relays in repetition coding.

In this work, we leverage the concept of network coding [27] to significantly improve the performance of the SCC scheme in a network of arbitrary size. In the technique that we propose, which is named superposition network coded cooperation (SNCC), a source node transmits its own information symbol superimposed with a relayed symbol by employing a power assignment. The relayed symbol is formed using bit-level operations [21, 28] over the previous symbols. The idea of network coding is used for a source node having detected more than one symbol from other source nodes in previous time slots and need to transmit all of them as relayed symbols together with its own symbol, using SCC. In this case, for more efficient power allocation, all relayed symbols are turned into one relayed symbol using bit-level Exclusive or (XOR) operations. This technique helps us have only two symbols, one source symbol and one relayed symbol, to transmit using SCC, rather than many symbols.

The SNCC scheme is applied to M-ary phase-shift keying (M-PSK) and M-ary quadrature amplitude modulation (M-QAM) modulation of the source symbols. It is shown that implementing the optimal receiver at the destination requires a high degree of complexity. Hence, a low-complexity sub-optimal approach for detection at the destination is proposed. This scheme is then analysed, and some good approximations on its performance are provided. We also compare the performance of SNCC with standard SCC and demonstrate the substantial role of network coding in performance improvement.

Finally, simulation results are presented. In comparison with the non-cooperative and the SCC scheme, SNCC does not require any additional time slots. The results show the superior performance of SNCC.

The rest of this paper is organised as follows. Section 2 provides the system model that is considered in the paper. The concept of SNCC and an approach for implementation of this technique are introduced. The structure of the receiver at the destination is presented in Section 3. The performance analysis follows in Section 4. In Section 5, we compare SNCC with SCC theoretically using a sub-optimal detection technique to demonstrate the advantages of SNCC in performance improvement. To verify the performance analysis, simulation results are presented in Section 6 and, finally, conclusions are drawn in Section 7.

2. SYSTEM MODEL

2.1. The concept of superposition network coded cooperation

A group consisting of n users is considered in a wireless network. The users, denoted by U_1, U_2, \dots, U_n , transmit information to a common destination in a TDMA manner. Every user is a source of information. In addition, users can operate as half-duplex relay nodes. The communication channels among the users and the destination are modelled as slow and flat Rayleigh fading with additive white Gaussian noise (AWGN) [1]. In this paper, it is assumed that the channel state information of a communication link is available at the receiver side. In practice, there are some ways for a receiver to obtain channel coefficients, that is, by sending a known sequence, called a pilot sequence, to the receiver [1].

The users are indexed according to their allocated time slot, so user $U_i, i = 1, 2, 3, \dots, n$, transmits during the i th time slot. Because of the propagation nature of wireless communications, the transmitted signal from U_i can be received by users $U_j, j > i$, that will transmit afterward. The received signal at user U_j from $U_i, j > i$ can be written as

$$y_{ij} = h_{ij}x_i + v_{ij}, \quad j = i + 1, \dots, n \quad (1)$$

where $h_{ij} \sim \mathcal{CN}(0, \sigma_{ij})$ is the channel coefficient between users U_i and U_j , and $v_{ij} \sim \mathcal{CN}(0, N_0)$ is zero-mean complex AWGN. The signal x_i , transmitted by user U_i , is

$$x_i = c_{1,i}s_i + \sqrt{1 - c_{1,i}^2}s_{1,\dots,i-1}, \quad i = 1, 2, \dots, n \quad (2)$$

where the symbol $s_i, i = 1, \dots, n$ is the source symbol of the i th user, whereas the superimposed symbol $s_{1,\dots,i-1}$ is information of previous users. The source symbols are chosen independently and equiprobably from an arbitrary M-ary constellation with average power $E[|s_i^2|] = a^2$. The

superposition coefficient $c_{1,i}$ is

$$c_{1,i} = \begin{cases} 1, & i = 1; \\ c_1, & i \neq 1 \end{cases} \quad (3)$$

and c_1 controls the amount of power assigned to the source and to the superimposed symbols transmitted by the i th user, $i > 1$. Setting $c_1 = 1$ simplifies our scheme to the non-cooperative scheme. As c_1 becomes smaller, the assigned power to the superimposed symbol increases. Clearly, the superimposed symbol causes interference to the source symbol. Hence, c_1 should be selected as close as possible to 1 for the disturbance to the source symbol to be as negligible as possible. The superimposed symbol $s_{1,\dots,i-1}$ is formed as

$$s_{1,\dots,i-1} = \mathcal{M}(s_1 \oplus s_2 \oplus \dots \oplus s_{i-1}) \quad (4)$$

where \oplus denotes bit-level XOR between two symbols and $\mathcal{M}(\cdot)$ is a mapping of the resulting bit sequence to a symbol from a constellation with the same average power (but not necessarily of the same type) as the source symbols. By acting as a decode-and-forward relay, each user can detect all required symbols to form the superimposed symbol. Finally, the received signal at the destination from user U_i is

$$y_i = h_i x_i + v_i, \quad i = 1, \dots, n \quad (5)$$

where the coefficient $h_i \sim \mathcal{CN}(0, \frac{1}{\lambda_i})$ is the channel between the i th user and the destination and v_i is zero-mean complex AWGN with variance N_0 .

According to the described model of SNCC, the required power to detect the information of previous users depends on the user, because for $i > j$, user U_i has to detect more information than user U_j . However, because in communication the transmission power is typically much higher than the reception power required by the receiver, we make the simplifying assumption that the reception power is negligible.

The transmission scheme is summarised in Table I. According to the model, the SNCC scheme requires no additional time slots compared with TDMA-based non-cooperative communication. This results in lower time delay than other TDMA-based cooperative strategies in which source and relay transmission phases take place in different time slots [18]. For such cooperative strategies (repetition coding being a well-known example), the required time slots for transmission are more than those of TDMA-based non-cooperative communication. In addition, synchronisation challenges for SNCC are not as

Table I. Transmission scheme in superposition network coded cooperation.

Transmission	U_1 Transmits	U_2 Transmits	U_3 Transmits	...	U_n Transmits
	s_1	(s_2, s_1)	$(s_3, s_1 \oplus s_2)$		$(s_n, s_1 \oplus s_2 \oplus \dots \oplus s_{n-1})$
Time slot	1	2	3	...	n

severe as those of simultaneous transmission-based cooperative protocols, because in SNCC, the users transmit in orthogonal time slots [18].

2.2. Implementation of SNCC

According to (2), the transmitted symbol of the i th user is formed using symbols s_1, s_2, \dots, s_i . In the following, we describe an approach to implement this scheme. When the transmission phase of user U_i is finished, the next users $U_j, i < j \leq n$ receive $y_{i,j}$ and, in the role of relay nodes, detect the source symbol s_i using an interference ignorant detector (II detector) given as [29]

$$\hat{s}_i = \arg \min_{s_i} |y_{i,j} - h_{i,j} c_{1,i} s_i| \quad (6)$$

which detects the desired symbol s_i by assuming the intentional interfering symbol $\sqrt{1 - c_{1,i}^2} s_{1,\dots,i-1}$ as Gaussian interference and ignoring its presence in the detection process. This approach provides low complexity for detection. However, the performance of the II detector is highly sensitive to interference. If the power of interference exceeds a specific threshold, an error floor in detection appears [29]. This error floor makes it impossible to achieve arbitrarily low error probability for detection, hence causing high degradation in detection performance [29]. Because the superimposed symbol appears as interference, the interference is controllable in SNCC. This means that the superimposed symbols can be designed so that the II detector have acceptable performance. To this end, we use the fact that two receivers with two different objectives will have the same performance if their decision regions for detecting a desired symbol are the same. We regulate the power of interference so that in detecting the source symbol s_i from $y_{i,j}$, the decision regions of the II detector be the same as the corresponding region of the optimal maximum-likelihood (ML) detector.

For M-PSK modulation of the source symbols, the superimposed symbol is chosen from a M-PAM constellation rotated by an angle equal to the phase of the source symbol s_i . Using this constraint, (2) can be written as

$$x_i = c_{1,i} s_i + \sqrt{1 - c_{1,i}^2} e^{j\varphi_{s_i}} s_{1,\dots,i-1}, \quad i = 1, 2, \dots, n \quad (7)$$

where $s_{1,\dots,i-1}$ is selected from a M-PAM constellation and φ_{s_i} is the phase of symbol s_i . By substituting the constellation points of M-PAM and M-PSK [30] in (7), the constellation points of all users, $U_i, 1 \leq i \leq n$, can be obtained as

$$\psi = \{\psi_{k,m}\} = \left\{ \left(c_{1,i} + A_m \sqrt{\frac{3(1 - c_{1,i}^2)}{M^2 - 1}} \right) a e^{j \frac{2\pi k}{M}} \right\} \quad (8)$$

$k, m = 1, 2, \dots, M$

where $A_m = 2m - 1 - M$. The average power of the constellation points in (8) is equal to

$$\begin{aligned} P_\psi &= \frac{1}{M^2} \sum_{k=1}^M \sum_{m=1}^M |\psi_{k,m}|^2 \\ &= \frac{a^2}{M} \left(M c_{1,i}^2 + \frac{3(1 - c_{1,i}^2)}{M^2 - 1} \sum_{m=1}^M A_m^2 \right) = a^2 \end{aligned} \quad (9)$$

Hence, the transmitted signal in the SNCC scheme has the same average power as that of the non-cooperative scheme. As shown in Appendix A, if we set

$$c_{1,i} + A_m \sqrt{\frac{3(1 - c_{1,i}^2)}{M^2 - 1}} > 0, \quad m = 1, 2, \dots, M \quad (10)$$

which is satisfied by $\sqrt{\frac{3}{4} \cdot \frac{M-1}{M-0.5}} \leq c_{1,i} < 1$, the II detector has the same performance as the ML detector in detecting the source symbol s_i from $y_{i,j}$. In summary, acceptable performance of the II detector can be guaranteed if the condition in (10) is met.

Similar approaches can be devised to implement SNCC for other source constellations. For M-QAM modulation of the source symbols, we can modulate the superimposed symbol using an M-QAM constellation with controllable power around the constellation points of the source symbol. This is equivalent to each user selecting its own transmitted symbol from a M^2 -QAM constellation ψ' as

$$\psi' = \{\psi'_{m,k} + j\psi'_{n,p}\} \quad (11)$$

where, for arbitrary n_1 and n_2

$$\psi'_{n_1, n_2} = \sqrt{\frac{3}{2(M-1)}} a \left(A'_{n_1} c_{1,i} + A'_{n_2} \sqrt{1 - c_{1,i}^2} \right) \quad (12)$$

and $A'_{n_i} = (2n_i - 1 - \sqrt{M})$. Same as in the M-PSK case, the average power of (12) is equal to that of the non-cooperative scheme. Also, by following a similar approach as in Appendix A, it can be easily seen that for

$$\sqrt{\frac{1 + M - 2\sqrt{M}}{2 + M - 2\sqrt{M}}} < c_{1,i} < 1 \quad (13)$$

the II and ML detectors have the same performance in detecting the source symbol s_i from $y_{i,j}$. As it is discussed in Section 6, an approximation of the optimal value for superposition coefficient can be obtained using numerical methods. However, there are some considerations in relation to selecting this coefficient. According to the modulation type, as $c_{1,i}$ approaches the lower bound in (10) or (13), the allocated power to relayed symbols increases, causing II detector performance to degrade. This highly

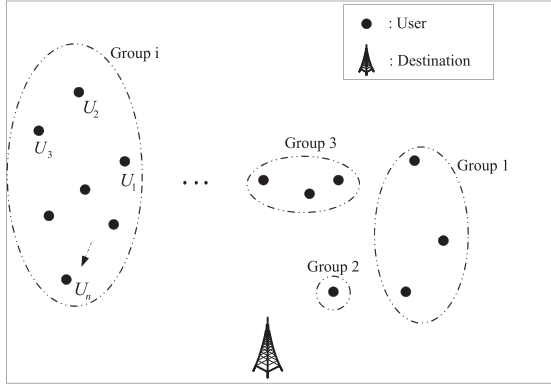


Figure 1. A wireless network with several users. The users are organised into groups of various members.

affects the communication performance in correctly detecting all the symbols. So we should select the superposition coefficient closer to the upper bound to obtain better performance. However, it should be considered that when $c_{1,i}$ gets very close to 1 (the upper bound), the effect of cooperation declines, because the power assigned to the relayed symbols decreases. In conclusion, considering its role in cooperation, we should select $c_{1,i}$ closer to the upper bound for a better communication performance.

In this model, it is assumed that the inter-user detection is an error-free process. Although performing the analysis

determine if it is able to detect the information of other users correctly. According to this method, a group may include fewer than or as many as N members. In this paper, indeed, we are describing SNCC for one of the groups, and we assume that it contains n users. This group is indicated in Figure 1 as Group i .

3. RECEIVER STRUCTURE AT THE DESTINATION

As we discussed previously, detection at each user loss in performance. In this section, we turn our attention to detection at the destination. Two different methods are proposed for detecting the symbols s_1, s_2, \dots, s_n from the received signals y_1, y_2, \dots, y_n , given in (5). The first approach is optimal detection, which gives rise to the best performance for the SNCC scheme at the cost of high complexity. To reduce the complexity, we propose a sub-optimal method for detection that renders the receiver implementation more practical.

3.1. Optimal detection

The optimal decision rule for detection is the maximum a posteriori probability rule, which, because of the equiprobability of source symbols in our scheme, reduces to the ML rule. In this case, the destination detects the symbol vector $\underline{s} = \{s_1, s_2, \dots, s_n\}$ from the received signal vector $\underline{y} = \{y_1, y_2, \dots, y_n\}$ as

$$\begin{aligned} \hat{\underline{s}} &= \arg \max_{\underline{s}} \left[f_{\underline{y}|\underline{s}}(\underline{y}|\underline{s}) \right] \\ &= \arg \max_{\underline{s}} \left[\exp \left(- \frac{\sum_{i=1}^n |y_i - h_i (c_{1,i}s_i + \sqrt{1 - c_{1,i}^2} g(s_i) s_{1,\dots,i-1})|^2}{N_0} \right) \right] \\ &= \arg \min_{\underline{s}} \left[\sum_{i=1}^n |y_i - h_i (c_{1,i}s_i + \sqrt{1 - c_{1,i}^2} g(s_i) s_{1,\dots,i-1})|^2 \right] \end{aligned} \quad (14)$$

under the assumption of non error-free inter-user channels is more realistic [31], but our analysis will be more complicated. Thus, every user $U_j, j = 2, \dots, n$ detects the information of all previous users $U_i, 1 \leq i < j$ correctly. In general, this assumption is not valid for all the users in a network because of the presence of channel fading and AWGN. However, there are some ways to segment the set of users in a network to some groups, as shown in Figure 1, so that users that are placed in a group detect the information of each other. Thereupon, by applying SNCC to each group separately, we can approach error-free inter-user detection. One way of making such a segmentation is by utilising cyclic redundancy check codes [32]. We consider a network composed of N users. The k -th member of the i -th group, $k \geq 1, i \geq 1$, is the first user that can detect the information transmitted by all previous users (up to user $k - 1$) in the i th group correctly and also is not a member of the previous groups (up to group $i - 1$) [32]. By using cyclic redundancy check codes, a user can

where $\hat{\underline{s}} = \{\hat{s}_1, \hat{s}_2, \dots, \hat{s}_n\}$ is the detected symbol vector and $f_{\underline{y}|\underline{s}}(\underline{y}|\underline{s})$ is the conditional probability density function (PDF) of vector \underline{y} given $\underline{s} = \underline{s}$. Also, $g(s_i)$ is equal to $e^{j\varphi_{s_i}}$ and 1 for M-PSK and M-QAM modulation, respectively. From (14), optimal detection for n users requires a search of order M^n , where M is the modulation order. Hence, the computational complexity of the optimal detector grows exponentially with n . This issue is a serious challenge for practical implementation of the receiver, especially for large numbers of cooperating users.

3.2. Practical sub-optimal detection

Because of the high complexity of the optimal receiver for SNCC, we propose a structure with lower complexity that exploits the benefits of SNCC. The proposed detection scheme is based on symbol error rate selection combining (SERS combining) [32] and successive interference cancellation (SIC) [29]. A SERS combiner selects the best

detection path among all available paths [32]. The criterion for selection is the SER. In other words, a SERS combiner selects the path with the lowest SER for detection. Because SERS combining is a sub-optimal detection method, the method proposed in this section has sub-optimal performance. To describe the approach, it is assumed that the n users transmit according to SNCC. The receiver uses y_1, \dots, y_n , given in (5), to detect the required symbols $\{s_1, \dots, s_n\}$. Each signal $y_i, i = 1, \dots, n$, includes two symbols s_i and $s_{1, \dots, i-1}$ according to (7). The symbol s_i can be detected by applying II detection to y_i directly. However, this method is not appropriate for detecting $s_{1, \dots, i-1}$, because the portion of power allocated to transmit s_i is much larger than that of $s_{1, \dots, i-1}$. So in order to detect $s_{1, \dots, i-1}$, the receiver must use SIC to remove the effect of s_i from y_i before applying the II detector. Using the signals y_1, \dots, y_n , it is possible for the receiver to detect every symbol in $\Psi_n = \{s_1, s_2, \dots, s_n, s_{1,1}, \dots, s_{1, \dots, n-1}\}$. Therefore, the set Ψ_n , comprising $2n - 1$ symbols, can be used by the receiver to detect the n symbols in the set $\phi_n = \{s_1, \dots, s_n\}$. In general, there may be several subsets of Ψ_n from which the symbols in ϕ_n can be obtained. As an example, consider the following five subsets of Ψ_3 of cardinality 3: $\varrho_3^1 = \{s_1, s_2, s_3\}$, $\varrho_3^2 = \{s_{1,1}, s_2, s_3\}$, $\varrho_3^3 = \{s_1, s_{1,2}, s_3\}$, $\varrho_3^4 = \{s_2, s_{1,2}, s_3\}$, and $\varrho_3^5 = \{s_{1,1}, s_{1,2}, s_3\}$. Using $s_1 = s_{1,1}$ and $s_{1,2} \oplus s_1 = s_2$, all the symbols in ϕ_3 can be extracted from each of the aforementioned sets. The problem for the receiver is to determine the best subset of Ψ_n that allows calculation of all the symbols in ϕ_n . To summarise, for a SERS combiner, the receiver must detect the symbols of a set ϱ_n of cardinality n satisfying the following conditions

- I- The detected symbols in ϱ_n are sufficient to obtain all the symbols in $\phi_n = \{s_1, \dots, s_n\}$.
- II- The set ϱ_n is the best subset of Ψ_n , $\Psi_n = \{s_1, s_2, \dots, s_n, s_{1,1}, \dots, s_{1, \dots, n-1}\}$, for correctly detecting all the symbols in ϕ_n , where best means that it corresponds to the path with the lowest SER for detection.

If Condition I is met, the detector will be able to obtain the symbols in ϕ_n from ϱ_n if the members of ϱ_n are correctly detected. This may be performed by bit-level XOR operations over the symbols in ϱ_n . Condition II ensures that the best ϱ_n for correctly detecting all the symbols in ϕ_n is selected. It can be easily shown that when Condition I is met, the probability of correct detection of all the symbols in ϕ_n using ϱ_n is equal to the probability of correct detection of all the symbols in ϱ_n . So Condition II can be described as finding ϱ_n so that for any other subset ϱ'_n of Ψ_n , satisfying Condition I we have

$$P_c^{\varrho_n}(\phi_n) \geq P_c^{\varrho'_n}(\phi_n) \quad (15)$$

where $P_c^{\varrho_n}(\phi_n)$ and $P_c^{\varrho'_n}(\phi_n)$ denote the probability of correctly detecting all the symbols in ϱ_n and ϱ'_n , respectively.

Before describing the detection algorithm for the general case, we introduce it using an example. For the three-user case, $n = 3$, the receiver has to find the best subset ϱ_3 of Ψ_3 , from which obtaining the symbols in ϕ_3 is feasible. As described previously, there are only five sets $\varrho_3^1, \varrho_3^2, \varrho_3^3, \varrho_3^4$ and ϱ_3^5 , that satisfy Condition I. According to the SERS combining method, the best set is the one with the highest probability of correct detection of all its elements. The simplest case of choosing the best set among two or more sets occurs when the sets are different only in one element. In other words, when the sets have $n - 1$ common elements and one different element. This, for example, holds for the sets ϱ_3^1, ϱ_3^2 (but not for ϱ_3^2, ϱ_3^3). In this case, the problem of finding the best set is simplified to finding the symbol with the highest probability of correct detection. As an example, the best set between ϱ_3^1 and ϱ_3^2 includes the symbols s_2 and s_3 , and its third element is one of the symbols s_1 or $s_{1,1}$ depending on which has the highest probability of correct detection. In order to determine the best set among $\varrho_3^1, \dots, \varrho_3^5$, we first find the best set $\varrho_{3,1}$ between ϱ_3^1 and ϱ_3^2 , we then find the best set $\varrho_{3,2}$ among ϱ_3^3, ϱ_3^4 and ϱ_3^5 , and we finally find the best set ϱ_3 between $\varrho_{3,1}$ and $\varrho_{3,2}$. According to the SERS combining method

$$\varrho_{3,1} = \begin{cases} \varrho_3^1, & \text{if } P_{cs_1} \cdot P_{cs_2} \cdot P_{cs_3} \geq P_{cs_{1,1}} \cdot P_{cs_2} \cdot P_{cs_3}, \\ \varrho_3^2, & \text{if } P_{cs_1} \cdot P_{cs_2} \cdot P_{cs_3} < P_{cs_{1,1}} \cdot P_{cs_2} \cdot P_{cs_3}, \end{cases} \quad (16)$$

which can be simplified as

$$\varrho_{3,1} = \begin{cases} \varrho_3^1, & \text{if } P_{cs_1} \geq P_{cs_{1,1}}, \\ \varrho_3^2, & \text{if } P_{cs_1} < P_{cs_{1,1}}, \end{cases} \quad (17)$$

where P_{cs_i} is the probability of correct detection of symbol s_i and $P_{cs_{1, \dots, i}}$ is the probability of correct detection of symbol $s_{1, \dots, i}$ conditioned on correct detection of s_{i+1} . With regard to the members of ϱ_3^1 and ϱ_3^2 , (17) can be written in compact form as

$$\varrho_{3,1} = \{\text{Sym}\{\text{Max}\{P_{cs_1}, P_{cs_{1,1}}\}\}, s_2, s_3\} \quad (18)$$

where the operator $\text{Max}\{\cdot\}$ selects the largest (maximum) value, and

$$\text{Sym}\{\text{Max}\{P_{cs_1}, P_{cs_{1,1}}\}\} = \begin{cases} s_1, & \text{if } \text{Max}\{P_{cs_1}, P_{cs_{1,1}}\} = P_{cs_1}, \\ s_{1,1}, & \text{if } \text{Max}\{P_{cs_1}, P_{cs_{1,1}}\} = P_{cs_{1,1}} \end{cases} \quad (19)$$

Similar to ϱ_3^1, ϱ_3^2 , the sets $\varrho_3^3, \varrho_3^4, \varrho_3^5$ have two common elements. Therefore, by following the same method, and using the fact that for an arbitrary user $i, i > 1$, $P_{cs_i} > P_{cs_{1, \dots, i-1}}$ always (because the larger portion of power is allocated to the source symbol s_i), after some simplifications, we have

$$\varrho_{3,2} = \begin{cases} \varrho_3^3, & \text{if } P_{cs_1} \geq P_{cs_2}, \\ \varrho_3^4, & \text{if } P_{cs_1} < P_{cs_2} \end{cases} \quad (20)$$

which can be written as

$$\varrho_{3,2} = \{\text{Sym}\{M_1\}, s_{1,2}, s_3\} \quad (21)$$

where $M_1 = \text{Max}\{P_{cs1}, P_{cs2}\}$, and

$$\text{Sym}\{M_1\} = \begin{cases} s_1, & \text{if } M_1 = P_{cs1}, \\ s_2, & \text{if } M_1 = P_{cs2} \end{cases} \quad (22)$$

A comparison between (18) and (21) reveals that the sets $\mathcal{Q}_{3,1}$ and $\mathcal{Q}_{3,2}$ do not have two common elements. However, because $P_{cs_i} > P_{cs1, \dots, i-1}$, (18) can also be written as

$$\mathcal{Q}_{3,1} = \{\text{Sym}\{M_1\}, \text{Sym}\{K_1\}, s_3\} \quad (23)$$

where $K_1 = \text{Med}\{P_{cs1}, P_{cs2}, P_{cs1,1}\}$, and $\text{Med}\{\cdot\}$ selects the second largest value (median of three values). Also,

$$\text{Sym}\{K_1\} = \begin{cases} s_1, & \text{if } K_1 = P_{cs1}, \\ s_2, & \text{if } K_1 = P_{cs2}, \\ s_{1,1}, & \text{if } K_1 = P_{cs1,1} \end{cases} \quad (24)$$

Now, the sets in (21) and (23) have two common elements. Thus, the best set \mathcal{Q}_3 between $\mathcal{Q}_{3,1}$ and $\mathcal{Q}_{3,2}$, which is also the best subset of Ψ_3 to obtain the symbols in ϕ_3 is

$$\mathcal{Q}_3 = \{\text{Sym}\{M_1\}, \text{Sym}\{M_2\}, s_3\} \quad (25)$$

where $M_2 = \text{Max}\{K_1, P_{cs1,2}\}$, and

$$\text{Sym}\{M_2\} = \begin{cases} s_1, & \text{if } M_2 = P_{cs1}, \\ s_2, & \text{if } M_2 = P_{cs2}, \\ s_{1,1}, & \text{if } M_2 = P_{cs1,1}, \\ s_{1,2}, & \text{if } M_2 = P_{cs1,2} \end{cases} \quad (26)$$

The aforementioned example gives the key idea behind the detection procedure. As shown in Appendix B, by

According to the detection approach, if the set \mathcal{Q}_n contains s_1, \dots, s_i , it certainly contains s_{i+1} . The receiver is composed of a SERS combiner, a successive interference canceller and an II detector. If the selected symbol is s_i , it is detected using the II detector and its effect is removed from y_i by SIC. After the removal operation, the II detector detects the symbol s_1, \dots, s_{i-1} , if it is selected. By the aforementioned procedure, the detection process becomes a step-by-step approach involving simple value comparisons. Therefore, by increasing the number of cooperating users, the complexity of the sub-optimal detection process increases linearly. This is the major advantage of the sub-optimal approach over the optimal case. This issue makes the implementation of the sub-optimal detector feasible.

4. ANALYSIS OF SNCC

In this section, the error performance of SNCC under the proposed sub-optimal detection scheme is analysed for M-PSK and M-QAM modulation. To this end, we find a good lower bound on the probability of correct detection for high signal to noise ratio (SNR). The results also make it possible to carry out a diversity analysis of SNCC.

According to the detection procedure, the probability of correctly detecting the first $n-1$ symbols in the set \mathcal{Q}_n (or equivalently the symbols s_1, \dots, s_{n-1}) can be evaluated as

$$P_c^{\mathcal{Q}_n} = \prod_{i=1}^{n-1} M_i \quad (27)$$

By referring to the detection procedure, M_i may be expanded as

$$M_i = \text{Max} \left\{ \underbrace{\text{Med}\{\dots \text{Med}\{P_{cs1}, P_{cs2}, P_{cs1,1}\}, \dots\}}_{i-1}, P_{cs_i}, P_{cs1, \dots, i-1}, P_{cs}^{i+1} \right\} \quad (28)$$

generalising the aforementioned method to an arbitrary number n , \mathcal{Q}_n can be obtained by steps shown in Table II.

where $P_{cs}^{i+1} = P_{cs_{i+1}}$ for $i = 1, \dots, n-2$ and $P_{cs}^n = P_{cs1, \dots, n-1}$. So in order to formulate $P_c^{\mathcal{Q}_n}$, expressions for P_{cs_k}

Table II. Calculation of \mathcal{Q}_n for any arbitrary number n .

Input: $P_{cs_i}, P_{cs1, \dots, i}, i = 1, \dots, n-1$
Output: \mathcal{Q}_n
1. Initialise: $K_0 = P_{cs1}$
2. for $i = 1 : n-2$
$M_i = \text{Max}\{K_{i-1}, P_{cs_{i+1}}\}$
$K_i = \text{Med}\{K_{i-1}, P_{cs_{i+1}}, P_{cs1, \dots, i}\}$
end
3. $M_{n-1} = \text{Max}\{K_{n-2}, P_{cs1, \dots, n-1}\}$
4. $\mathcal{Q}_n = \{\text{Sym}\{M_1\}, \dots, \text{Sym}\{M_{n-1}\}, s_n\}$
$\text{Sym}\{M_i\}$ selects a symbol s from Ψ_{i+1} so that $P_{cs} = M_i, s \neq \{\text{Sym}\{M_1\}, \text{Sym}\{M_2\}, \dots, \text{Sym}\{M_{i-1}\}, s_n\}$.

and $P_{CS_1, \dots, k}, k = 1, \dots, n-1$ must be acquired. As shown in Appendix C, the following are good lower bounds for P_{CS_k} and $P_{CS_1, \dots, l}$

$$\begin{aligned} P_{CS_k} &> 1 - \xi \sum_{m=1}^{M'} Q\left(u_m \sqrt{2|h_i|^2 \text{SNR}}\right), \text{ and} \\ P_{CS_1, \dots, l} &> 1 - \xi \sum_{m=1}^{M'} Q\left(v_m \sqrt{2|h_{l+1}|^2 \text{SNR}}\right) \end{aligned} \quad (29)$$

where $\text{SNR} = \frac{a^2}{N_0}$. The expressions for M-PSK modulation are obtained by making the following substitutions in (29)

$$\begin{aligned} M' &= M, \quad \xi = \frac{2}{M}, \\ u_m &= \left(c_1 + A_m \sqrt{\frac{3(1-c_1^2)}{M^2-1}} \right) \sin\left(\frac{\pi}{M}\right), \text{ and} \\ v_m &= \frac{\sqrt{3(1-c_1^2)}}{\sqrt{M^2-1} \sin\left(\frac{\pi}{M}\right)} u_m \end{aligned} \quad (30)$$

whereas, for M-QAM,

$$\begin{aligned} M' &= \sqrt{M}, \quad \xi = \frac{4}{\sqrt{M}} \left(1 - \frac{1}{\sqrt{M}}\right), \\ u_m &= \sqrt{\frac{3}{2(M-1)}} \left(c_1 + A'_m \sqrt{1-c_1^2} \right), \text{ and} \\ v_m &= \sqrt{1-c_1^2} u_m \end{aligned} \quad (31)$$

Thus, the lower bounds for $P_c^{Q_n}$ for M-PSK and M-QAM can be obtained from (27)–(29). The next step is to calculate the average value of the expression in (27). To the best of our knowledge, there is not any known expression for the probability density function (PDF) of the random functions M_i . However, because the Q-function is monotonically decreasing, substituting the bounds in (29) into (28) yields

$$M_i > 1 - \xi \sum_{m=1}^{M'} Q\left(\sqrt{2 \cdot \Gamma_{i,m} \text{SNR}}\right) \quad (32)$$

where

$$\Gamma_{i,m} = \text{Max} \left\{ \underbrace{\text{Med}\{\dots \text{Med}\{\gamma_{1,m}, \gamma_{2,m}, \gamma_{2,m}, \dots\}, \dots\}}_{i-1}, \gamma_{i,m}, \zeta_{i,m}, \gamma_m^{i+1} \right\} \quad (33)$$

$\gamma_{i,m} = u_m^2 |h_i|^2$, $\zeta_{i,m} = v_m^2 |h_i|^2$, $\gamma_m^n = \zeta_{n,m}$, and for $i = 1, \dots, n-2$, $\gamma_m^{i+1} = \gamma_{i+1,m}$. By substituting (32)

in (27) and noting that the product of two or more Q-functions with large arguments is negligible in comparison with their sum, we obtain a lower bound for $P_c^{Q_n}$ as

$$P_c^{Q_n} > 1 - \xi \sum_{m=1}^{M'} \sum_{i=1}^{n-1} Q\left(\sqrt{2 \cdot \Gamma_{i,m} \text{SNR}}\right) \quad (34)$$

It is possible to derive an expression for $E[P_c^{Q_n}]$, ($E[\cdot]$ denotes the expectation), if the PDF of $\Gamma_{i,m}$ is available. We now find the distribution of $\Gamma_{i,m}$ for a specific m . To improve the readability, from now on, the index m is omitted unless is necessary. From (33), $\Gamma_i = \text{Max}\{\Lambda_i, \gamma^{i+1}\}$, where $\Lambda_i = \text{Med}\{\Lambda_{i-1}, \gamma_i, \alpha \gamma_i\}$, $\alpha = \frac{\zeta_i}{\gamma_i} = \frac{v_m^2}{u_m^2} < 1$ and $\Lambda_1 = \gamma_1$. The cumulative density function of Λ_i is

$$\begin{aligned} F_{\Lambda_i}(x) &= P\{\Lambda_i < x\} = \int_0^x \int_{x_1}^{\frac{1}{\alpha} x_1} f_{\Lambda_{i-1}, \gamma_i}(x_1, x_2) dx_2 dx_1 \\ &+ \int_0^x \int_{x_2}^{\infty} f_{\Lambda_{i-1}, \gamma_i}(x_1, x_2) dx_1 dx_2 \\ &+ \int_0^{\frac{x}{\alpha}} \int_0^{\alpha x_2} f_{\Lambda_{i-1}, \gamma_i}(x_1, x_2) dx_1 dx_2 \end{aligned} \quad (35)$$

where $P\{\cdot, \cdot\}$ and $f(\cdot, \cdot)$ denote the joint probability function and joint PDF, respectively. Because Λ_{i-1} and γ_i are independent, (35) is easy to evaluate. Then the distribution of Λ_i can be shown to be

$$\begin{aligned} F_{\Lambda_i}(x) &= (1 - F_{\Lambda_{i-1}}(x)) \left(1 - F_{\gamma_i}\left(\frac{x}{\alpha}\right)\right) \\ &- (1 - F_{\Lambda_{i-1}}(x)) (1 - F_{\gamma_i}(x)) + F_{\gamma_i}\left(\frac{x}{\alpha}\right) \end{aligned} \quad (36)$$

Because γ_i is an exponential random variable with mean $\frac{u_m^2}{\lambda_i}$, (36) can be written as

$$\begin{aligned} 1 - F_{\Lambda_i}(x) &= (1 - F_{\Lambda_{i-1}}(x)) e^{-\lambda'_i x} \\ &- (1 - F_{\Lambda_{i-1}}(x)) e^{-\frac{\lambda'_i}{\alpha} x} + e^{-\frac{\lambda'_i}{\alpha} x} \end{aligned} \quad (37)$$

where $\lambda'_i = \frac{\lambda_i}{u_m^2}$, $i = 1, \dots, n-1$. From (37), the distribution of Λ_i depends on the distribution of Λ_{i-1} . So (37) is a recursive equation with initial term $F_{\Lambda_1}(x) = 1 - e^{-\lambda_1 x}$. By solving (37) for $i = 2, 3, \dots$, it is found that for arbitrary i the term $1 - F_{\Lambda_i}(x)$ is composed of a sum of $2^i - 1$ exponential terms as

$$1 - F_{\Lambda_i}(x) = \sum_{k=1}^{2^i-1} (-1)^{k+1} e^{-\lambda^{k,i} x} \quad (38)$$

where $\lambda^{k,1} = \lambda'_1$. To obtain a recursive form for $\lambda^{k,i}$, $i > 1$, (37) has to be solved using (38). By substituting (38) in

(37) we have

$$\sum_{k=1}^{2^i-1} (-1)^{k+1} e^{-\lambda^{k,i} x} = \left(\sum_{k=1}^{2^{i-1}-1} (-1)^{k+1} e^{-(\lambda^{k,i-1} + \lambda'_i)x} \right) - \left(\sum_{k=1}^{2^{i-1}-1} (-1)^{k+1} e^{-\left(\lambda^{k,i-1} + \frac{\lambda'_i}{\alpha}\right)x} \right) + e^{-\frac{\lambda'_i}{\alpha} x} \quad (39)$$

Now, by expanding the left hand side term of (39) as

$$\sum_{k=1}^{2^i-1} (-1)^{k+1} e^{-\lambda^{k,i} x} = \left(\sum_{k=1}^{2^{i-1}-1} (-1)^{k+1} e^{-(\lambda^{k,i} x)} \right) - \left(\sum_{k=2^i}^{2^{i-2}} (-1)^k e^{-(\lambda^{k,i} x)} \right) + e^{-\lambda^{2^i-1} x} \quad (40)$$

and comparing (39) with (40), the following recursive formula is obtained

$$\lambda^{k,i} = \begin{cases} \lambda^{k,i-1} + \lambda'_i, & \text{if } 1 \leq k \leq 2^{i-1} - 1, \\ \lambda^{[k],i-1} + \left(\frac{\lambda'_i}{\alpha}\right), & \text{if } 2^{i-1} \leq k \leq 2^i - 2, \\ \frac{\lambda'_i}{\alpha}, & \text{if } k = 2^i - 1 \end{cases} \quad (41)$$

where $[k] = k + 1 - 2^{i-1}$. According to (41), for a specific i , $\lambda^{k,i}$ is a linear combination of λ'_j , $j = 1, \dots, i$. On the other hand, λ'_j is proportional to the reciprocal of the j -th user's channel variance. So the exponents of the exponential terms in (38) are linear combinations of the reciprocal of the first i users' channel variances. Because Λ_i and γ^{i+1} are independent, the distribution of Γ_i can be written as

$$F_{\Gamma_i}(x) = P\{\Lambda_i < x, \gamma^{i+1} < x\} = F_{\Lambda_i}(x) F_{\gamma^{i+1}}(x) \quad (42)$$

By substituting the cumulative density function of Λ_i and γ^{i+1} in (42), the distribution of Γ_i is achieved as

$$F_{\Gamma_i}(x) = \left(1 - \sum_{k=1}^{2^i-1} (-1)^{k+1} e^{-\lambda^{k,i} x} \right) \cdot \left(1 - e^{-\lambda'_{i+1} x} \right) \quad (43)$$

where $\lambda'_n = \frac{\lambda_n}{v_n^2}$. Differentiating (43) with respect to x yields the PDF of Γ_i as

$$f_{\Gamma_i}(y) = \lambda'_{i+1} e^{-\lambda'_{i+1} y} + \sum_{k=1}^{2^i-1} (-1)^{k+1} \left(\lambda^{k,i} e^{-\lambda^{k,i} y} - \left(\lambda^{k,i} + \lambda'_{i+1} \right) e^{-(\lambda^{k,i} + \lambda'_{i+1}) y} \right) \quad (44)$$

As mentioned before, although the index m is omitted, $\lambda^{k,i}$ and λ'_{i+1} are functions of m . So $\lambda^{k,i}$ and λ'_{i+1} should be denoted as $\lambda_m^{k,i}$ and $\lambda'_{i+1,m}$, respectively, when it is necessary to show their dependence on m .

In order to calculate the average value for the lower bound of $P_c^{Q_n}$ given in (34), we consider the Taylor

expansion of the well-known expression for average probability of error [1] as

$$E \left[Q \left(\sqrt{k \text{SNR} \cdot X} \right) \right] = - \sum_{n=1}^{\infty} \left(\frac{1}{2n!} \left(\frac{2\lambda_x}{k \text{SNR}} \right)^n \prod_{i=1}^n \left(\frac{1}{2} - i \right) \right) \quad (45)$$

where k is a constant, X is an exponential random variable with mean $\frac{1}{\lambda_x}$ and the Taylor expansion is calculated at $\frac{\lambda_x}{k \text{SNR}} = 0$. By utilising (45), the lower bound for the average value of $P_c^{Q_n}$ for high SNR, after some simplifications may be expressed as

$$E \left[P_c^{Q_n} \right] > 1 - \frac{3\xi}{8 \text{SNR}^2} \sum_{m=1}^{M'} \sum_{i=1}^{n-1} \sum_{k=1}^{2^i-1} \left((-1)^{k+1} \lambda_m^{k,i} \lambda'_{i+1,m} \right) + O \left(\frac{1}{\text{SNR}^3} \right) \quad (46)$$

Finally, from (41), we have $\sum_{k=1}^{2^i-1} ((-1)^{k+1} \lambda^{k,i}) = \lambda'_i$, so (46) is simplified to

$$E \left[P_c^{Q_n} \right] > 1 - \frac{3\xi}{8 \text{SNR}^2} \sum_{m=1}^{M'} \sum_{i=1}^{n-1} \lambda'_{i,m} \lambda'_{i+1,m} + O \left(\frac{1}{\text{SNR}^3} \right) \quad (47)$$

which shows a diversity order 2. From (29) and (45), for the last symbol, s_n , we have

$$E \left[P_{c s_n} \right] > 1 - \frac{\xi \lambda_n}{4 \text{SNR}} \sum_{m=1}^{M'} \frac{1}{u_m^2} + O \left(\frac{1}{\text{SNR}^2} \right) \quad (48)$$

Therefore, the diversity order of the last symbol is 1.

Depending on the values in (30) and (31), the expressions in (47) and (48) are valid for M-PSK and M-QAM modulation, respectively.

5. PERFORMANCE COMPARISON OF SCC AND SNCC

In this section, an analytical performance comparison between SNCC and the standard SCC schemes is provided when both schemes use sub-optimal method of Section 3.2 for detection, the two schemes can be compared directly because of their equal transmission time. In addition, the comparison demonstrates the important role of network coding in obtaining considerable performance improvement.

The SNCC model, which was described in Section 2, can be reduced to the standard SCC scheme if the bit-level XOR operations are omitted. In other words, by replacing s_1, \dots, s_{i-1} with $s'_{i-1} = s_{i-1}$ in our proposed model, the transmission model for the SCC scheme is obtained. With this replacement, (14) provides the optimal detection method

for SCC. Also, in this case the procedure for sub-optimal detection at the destination is simplified to

$$\begin{aligned} LB_{SNCC} &= 1 - \frac{3\xi}{8\text{SNR}^2} \sum_{m=1}^{M'} \left(\frac{\lambda_1 \lambda_2}{u_m^4} + \frac{\lambda_2 \lambda_3}{u_m^4} + \dots + \frac{\lambda_{n-2} \lambda_{n-1}}{u_m^4} + \frac{\lambda_{n-1} \lambda_n}{u_m^2 v_m^2} \right) + O\left(\frac{1}{\text{SNR}^3}\right), \\ LB_{SCC} &= 1 - \frac{3\xi}{8\text{SNR}^2} \sum_{m=1}^{M'} \left(\frac{\lambda_1 \lambda_2}{u_m^2 v_m^2} + \frac{\lambda_2 \lambda_3}{u_m^2 v_m^2} + \dots + \frac{\lambda_{n-2} \lambda_{n-1}}{u_m^2 v_m^2} + \frac{\lambda_{n-1} \lambda_n}{u_m^2 v_m^2} \right) + O\left(\frac{1}{\text{SNR}^3}\right) \end{aligned} \quad (53)$$

- 1: *for* $i = 1 : n - 1$
 $N_i = \text{Max}\{P_{cs_i}, P_{cs'_i}\}$
end
- 2: $\rho_n = \{\text{Sym}\{N_1\}, \dots, \text{Sym}\{N_{n-1}\}, s_n\}$,

where the set ρ_n , the best set for detecting all required symbols, P_{cs_i} , is defined as before and $P_{cs'_i}$ is the probability of correct detection of s'_i conditioned on correct detection of s_{i+1} . For this detection method, the probability of correctly detecting the symbols $\{s_1, \dots, s_{n-1}\}$ can be evaluated as

$$P_c^{\rho_n} = \prod_{i=1}^{n-1} N_i \quad (49)$$

The lower bounds in (29) are valid for P_{cs_i} and $P_{cs'_i}$ because the SCC scheme is a simplified form of SNCC with $s_{1,\dots,l}$ replaced by s'_l . Therefore, using the same detection method and the same reasoning as for SNCC, a good lower bound for $P_c^{\rho_n}$ is

$$P_c^{\rho_n} > 1 - \xi \sum_{m=1}^{M'} \sum_{i=1}^{n-1} Q\left(\sqrt{2 \cdot \Theta_{i,m} \text{SNR}}\right) \quad (50)$$

With the same definitions for $\gamma_{i,m}$ and $\zeta_{i,m}$ as for SNCC, $\Theta_{i,m} = \text{Max}\{\gamma_{i,m}, \zeta_{i+1,m}\}$. Because $\gamma_{i,m}$ and $\zeta_{i+1,m}$ are independent, the distribution of $\Theta_{i,m}$ can simply be calculated as

$$\begin{aligned} f_{\Theta_{i,m}}(y) &= \lambda'_{i,m} e^{-\lambda'_{i,m} y} + \lambda''_{i+1,m} e^{-\lambda''_{i+1,m} y} \\ &\quad - (\lambda'_{i,m} + \lambda''_{i+1,m}) e^{-(\lambda'_{i,m} + \lambda''_{i+1,m}) y} \end{aligned} \quad (51)$$

where $\lambda'_{i,m} = \frac{\lambda_i}{u_m^2}$ and $\lambda''_{i,m} = \frac{\lambda_i}{v_m^2}$. Using (45) and averaging both sides of (50) over the distribution in (51) yields

$$E[P_c^{\rho_n}] > 1 - \frac{3\xi}{8\text{SNR}^2} \sum_{m=1}^{M'} \sum_{i=1}^{n-1} \lambda'_{i,m} \lambda''_{i+1,m} + O\left(\frac{1}{\text{SNR}^3}\right) \quad (52)$$

which holds for M-PSK and M-QAM, using (30) and (31), respectively. It can be easily found that (48) is valid for s_n in the SCC case.

From the results of the analysis, we can compare SNCC and SCC when the sub-optimal SERS combining method is used for detection. For the last symbol, s_n , SNCC and SCC have the same error performance. However, for the remaining symbols, s_1, \dots, s_{n-1} , the performance of SNCC is

significantly better than SCC. To support this claim, we expand the lower bounds in (47) and (52) as

Considering (30) and (31), it can be easily seen that for $c_1 > 0$, $u_m > v_m$. A comparison between LB_{SNCC} and LB_{SCC} in (53) makes it clear that for $u_m > v_m$, the error probability of SNCC is smaller than that of SCC. Furthermore, from (10) and (13), the coefficient c_1 must be selected close to 1. This constraint causes u_m to be significantly larger than v_m . Therefore, choosing $c_{1,i}$ close to 1 renders the performance of SNCC much better than SCC.

As described before, the optimal detector implementation has high complexity. So the analytical comparison in this section provides a comparison from a practical viewpoint. In the Section 6, a comparison between SNCC and SCC is provided when the optimal detection method is used. The simulation results show that even when the sub-optimal detector is used, the performance of SNCC is better than the performance of SCC when the optimal receiver is employed.

6. SIMULATION RESULTS

In this section, computer simulations are presented to validate the analytical results and to demonstrate the performance improvement compared with SCC and the non-cooperative scheme. In this part, user-destination channel is modelled as narrow-band Rayleigh fading with AWGN. For all users, the average transmit power is a^2 , and the noise variance is N_0 . The figures show the SER performance as a function of $\text{SNR} = \frac{a^2}{N_0}$, where by setting $N_0 = 1$, we have SER as a function of average transmit power, a^2 .

Figure 2 presents a performance comparison of different communication schemes for specific channel realisations. The figure shows the SER performance versus the SNR for 5 users, 4-QAM modulation of source symbols, $|h_1| = 0.191$, $|h_2| = 0.094$, $|h_3| = 1.077$, $|h_4| = 2.86$, and $|h_5| = 0.17$. In other words, by fixing channel coefficients $h_i, i = 1, \dots, 5$ to some constant values, and having additive noise as a random variable, the SER performance in a specific SNR is an average term over different noise realisations. The values of $h_i, i = 1, \dots, 5$ are chosen in a random manner using a Gaussian random number generator. Also, $c_1 = 0.99$ is selected for the SCC and SNCC schemes, and the sub-optimal algorithm is used for detection. The aim of this simulation is to give a better view of the proposed sub-optimal detection algorithm and the paths that it selects to detect the desired symbols. A comparison between the curves reveals that the SNCC and the non-cooperative schemes have the best and the worst performance at all SNRs, respectively. For the

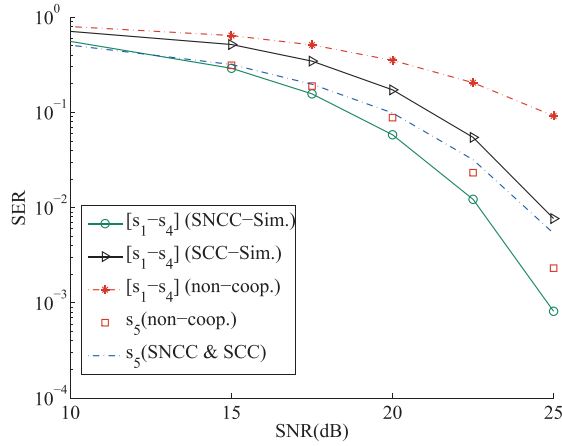


Figure 2. Symbol Error Rate (SER) performance versus signal to noise ratio (SNR) for specific channel realisations for five users, 4-QAM modulation of the source symbols, the sub-optimal detection method for superposition coded cooperation (SCC) and superposition network coded cooperation (SNCC), $c_1 = 0.99$, $|h_1| = 0.191$, $|h_2| = 0.094$, $|h_3| = 1.077$, $|h_4| = 2.86$, and $|h_5| = 0.17$.

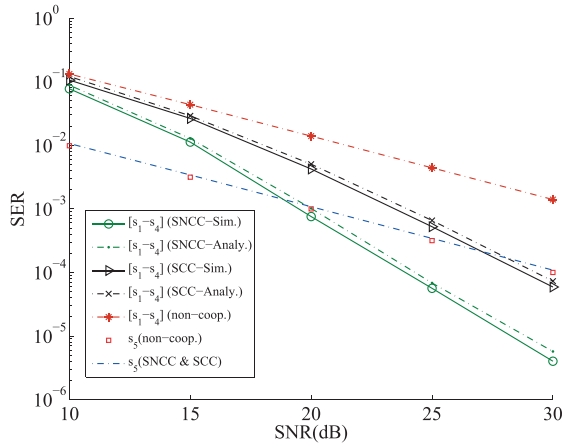


Figure 3. Symbol Error Rate (SER) performance versus signal to noise ratio (SNR) for five users, 4-QAM modulation of the source symbols, the sub-optimal detection method for superposition coded cooperation (SCC) and superposition network coded cooperation (SNCC), $c_1 = 0.99$, $\lambda_1 = 0.5$, $\lambda_2 = 0.4$, $\lambda_3 = 0.3$, $\lambda_4 = 0.2$, and $\lambda_5 = 0.1$.

non-cooperative scheme there is always one choice for detection. In other words, this scheme can only detect symbols $\{s_1, s_2, s_3, s_4, s_5\}$. However, because the channel value for the second user U_2 is small, there is a better choice for SCC. The detection path for SCC includes the symbols $\rho_5 = \{s_1, s_{1,2}, s_3, s_4, s_5\}$. For SNCC there is an even better detection path. The best path for SNCC is $\rho_5 = \{s_1, s_3, s_{1,2,3}, s_4, s_5\}$. Therefore, the higher degree of freedom for SNCC to select the best path renders its performance better than the other schemes. Because average

SER is an average term over many channel realisations, this simulation provides a better insight into why SNCC has a better performance in terms of average SER.

In the following figures channel coefficients $h_i, i = 1, \dots, 5$ are complex Gaussian random variables with variance $\frac{1}{\lambda_i}$, and the SER performance in a specific SNR is an average term over different channel and noise realisations. Obviously, a larger λ_i means a smaller channel variance or equivalently worse channel condition. We have selected $\lambda_1 \geq \lambda_2 \geq \dots \geq \lambda_5$ for all simulations to satisfy the system model assumption, in which it was supposed that a user with worse channel coefficient (larger λ_i) transmits earlier.

The SER performance versus the SNR for 5 users with $\lambda_1 = 0.5$, $\lambda_2 = 0.4$, $\lambda_3 = 0.3$, $\lambda_4 = 0.2$, $\lambda_5 = 0.1$, and 4-QAM modulation of the source symbols is depicted in Figure 3. We choose the superposition factor $c_1 = 0.99$. In this example the proposed sub-optimal detection method is used for both SCC and SNCC. The excellent agreement between the simulation and analytical results demonstrates the accuracy of our analysis for SNCC. By comparing the performance of SNCC with the non-cooperative scheme the superiority of SNCC in detecting the information of the first four users at all SNRs can be confirmed. This performance improvement increases significantly with the SNR. For SNR = 20 dB the error probability of SNCC is about 19 times smaller than that of the non-cooperative scheme. This advantage is achieved by SNCC without any additionally time slot requirements. However, for the last user, not only the performance has not improved, but also a small degradation can be observed. This degradation is expected, because the last user allocates a portion of its own power to transmit information of other users. Moreover, the information in s_n is not sent by any other users. However, as shown in the figure, the degradation is negligible. In general, the degradation in the SER performance of the last user can be made arbitrarily small by choosing the superposition factor c_1 sufficiently close to 1. On the other hand, by selecting c_1 excessively close to 1, the cooperative advantage of SNCC for other users tends to vanish. This exhibits a trade-off between the performance degradation of the last user and the improvement of the others. Therefore, it is important to choose the factor c_1 in an efficient manner to gain acceptable performance improvement for the first $n - 1$ users without significant degradation in the performance of the last user. Figure 3 also provides a comparison between SNCC and SCC. The performance gain of SNCC over SCC demonstrates the important role of network coding here. In fact, SNCC and SCC are identical in all aspects with the exception of the use of network coding by SNCC. Therefore, using network coding has resulted in reducing the SER by a factor of 6 at SNR = 20 dB.

Figure 4 provides a performance comparison among different communication strategies for five users with $\lambda_1 = 0.02$, $\lambda_2 = 0.018$, $\lambda_3 = 0.016$, $\lambda_4 = 0.015$, and $\lambda_5 = 0.014$, and superposition factor $c_1 = 0.995$. In this case, 16-QAM modulation is used for communication, and the sub-optimal detection method is applied to SCC and SNCC. From (13), as the modulation order increases,

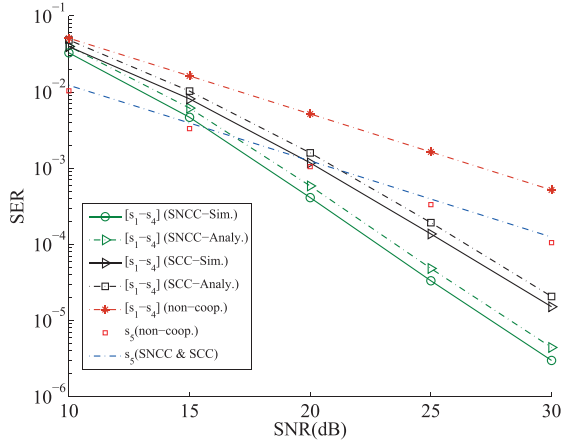


Figure 4. Symbol error rate (SER) performance versus signal to noise ratio (SNR) for five users, 16-QAM modulation of the source symbols, the sub-optimal detection method for superposition coded cooperation (SCC) and superposition network coded cooperation (SNCC), $c_1 = 0.995$, $\lambda_1 = 0.02$, $\lambda_2 = 0.018$, $\lambda_3 = 0.016$, $\lambda_4 = 0.015$, and $\lambda_5 = 0.014$.

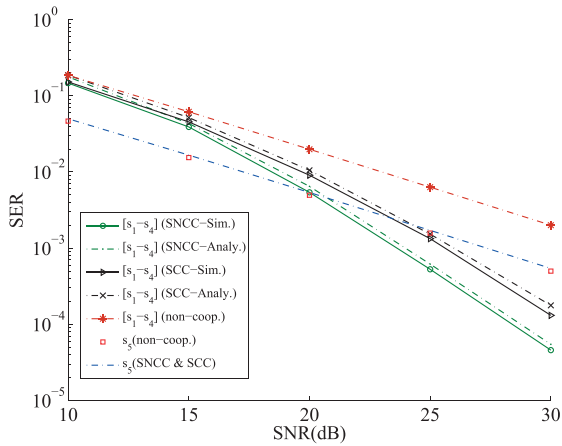


Figure 5. Symbol error rate (SER) performance versus signal to noise ratio (SNR) for five users, 4-QAM modulation of the source symbols, the sub-optimal detection method for superposition coded cooperation (SCC) and superposition network coded cooperation (SNCC), $c_1 = 0.99$, and $\lambda_1 = \lambda_2 = \lambda_3 = \lambda_4 = \lambda_5 = 0.5$.

the acceptable range for c_1 gets smaller. This range is between 0.95 and 1 for 16-QAM modulation. However, as can be seen from Figure 4, by allocating only 1 per cent of the power of a user to the superimposed symbol, the overall performance of communication can be improved significantly.

A special case for our model occurs when all the users in the network tend to have the same channel variances. Figure 5 presents the SER performance versus the SNR for the same scenario as Figure 3, when $\lambda_i = 0.5$, $i = 1, \dots, 5$,

and the sub-optimal detection method is used for SCC and SNCC. This figure reveals the advantages of SNCC in comparison with direct transmission and SCC, even for this special scenario.

A performance comparison between the optimal and the sub-optimal detection methods for both SCC and SNCC is shown in Figure 6. As can be seen, for both schemes, the optimal detector results in better performance at the cost of higher complexity compared with the sub-optimal detector. However, the same slope of the SER curves at high SNR proves that the same diversity order is achieved by all detectors. Also, by comparing SNCC and SCC curves, it can be deduced that the performance of SNCC when the suboptimal receiver is used is better than the performance of SCC even if the optimal receiver is employed.

Figure 7 depicts the SER performance of the users for the same scenario as Figure 3 for different values of c_1 at SNR = 25 dB, when the proposed sub-optimal detection method is used for both SCC and SNCC. As can be seen in the figure, the SER variation versus c_1 for the first four users in the SNCC scheme is not monotonic. In other words, by moving from $c_1 = 1$ towards $c_1 = 0.9$, the SER reduces at first, with a large slope. This slope gets smaller as c_1 is reduced further. Finally, when c_1 approaches 0.9, the SER increases. Allocating power to superimposed symbols results in significant performance improvement because it creates the opportunity of cooperation among users. However, increasing the power allocated to the superimposed symbols also increases the interference to source symbols. Therefore, arbitrary reduction of c_1 in its acceptable range, does not lead to better performance. The best performance for the first $n - 1$ users can be achieved by selecting c_1 at a reasonable distance from 1. From Figure 7, it can be observed that selecting $c_1 =$

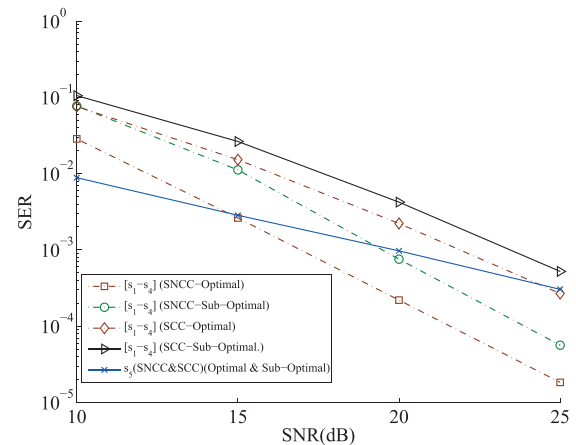


Figure 6. Performance comparison between superposition coded cooperation (SCC) and superposition network coded cooperation (SNCC) when the optimal and the sub-optimal detection methods are used, for five users, 4-QAM modulation of the source symbols, $c_1 = 0.99$, $\lambda_1 = 0.5$, $\lambda_2 = 0.4$, $\lambda_3 = 0.3$, $\lambda_4 = 0.2$, and $\lambda_5 = 0.1$.

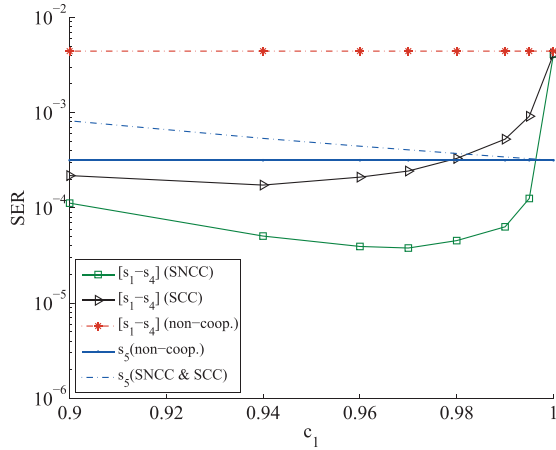


Figure 7. Symbol error rate (SER) performance versus the superposition factor c_1 , for five users with 4-QAM modulation of the source symbols, the sub-optimal detection method for superposition coded cooperation (SCC) and superposition network coded cooperation (SNCC), $\lambda_1 = 0.5$, $\lambda_2 = 0.4$, $\lambda_3 = 0.3$, $\lambda_4 = 0.2$, and $\lambda_5 = 0.1$, SNR = 25dB.

0.97 provides better performance for all users than when $c_1 = 0.9$ is selected. In general, to obtain the optimal value for c_1 at a specific SNR, we need the probability of correctly detecting all symbols s_1, \dots, s_n as a function of c_1 . The analytical terms for SNCC, given in Section 3, are not exact. So the optimal value for c_1 cannot be obtained analytically. However, as the terms give good approximations of the error performance, we can utilise them to determine some near-optimal values for c_1 . By multiplying the lower bounds in (47) and (48) together, an approximate function for the probability of correct detection of all symbols s_1, \dots, s_n can be obtained. By differentiating this function with respect to c_1 , it becomes clear that there is not an analytical solution for c_1 that makes the differentiated function equal to zero. Therefore, the near-optimal value for c_1 can only be obtained by numerical methods.

Figure 8 is provided to give an insight into the effect of the number of cooperating users on the SER performance. This figure demonstrates the SER performance for the same scenario as Figure 3 and two cases: (i) when only the first three users transmit to the destination and (ii) when all five users transmit. Sub-optimal detection methods are used for both SCC and SNCC. By comparing the curves, we find that the SER performance of SNCC for the first four users in the five-user case is significantly better than the SER performance of the first two users in the three-user case. However, the opposite is true for SCC and the non-cooperative scheme. This leads us to an important observation. In general, by increasing n , the probability of correctly detecting the information of the first $n - 1$ users always reduces in SCC and non-cooperative schemes, while in some cases such as this scenario, it can increase in the SNCC scheme. This advantage is achieved by SNCC because of fairly utilising the channel conditions of some users to improve the performance of other worse users.

Finally, Figure 9 provides a performance comparison between QAM and PSK modulation of source symbols for the same scenario as Figure 3. The sub-optimal detection approaches are used for both SCC and SNCC. Although for non-cooperative communication, 4-PSK and 4-QAM modulation have the same error performance, changing the constellation type of the superimposed symbols in the PSK case results in the performance of SNCC for QAM being always better than that of PSK. Because, in general, QAM has better error performance than that of PSK, it is anticipated that the difference between the SER performance of SNCC for QAM and PSK modulation will become even larger by increasing the modulation order.

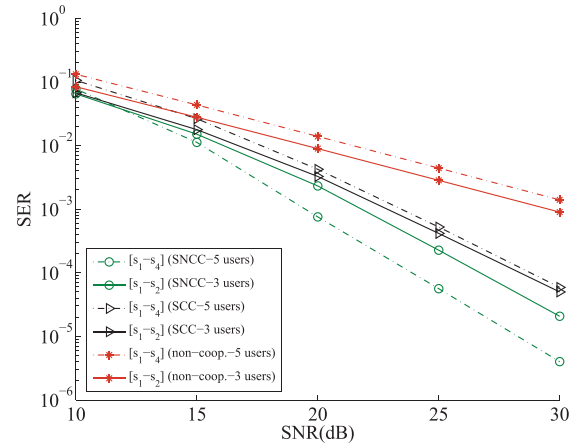


Figure 8. Symbol error rate (SER) performance versus signal to noise ratio (SNR), for two cases: 1- the first three users and 2- all the users in Figure 3 transmit to destination, the sub-optimal detection method for superposition coded cooperation (SCC) and superposition network coded cooperation (SNCC).

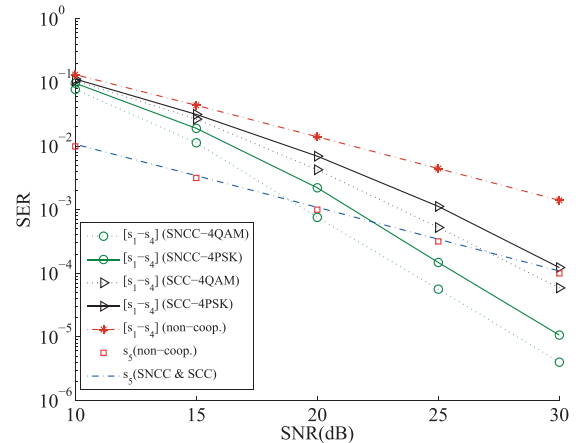


Figure 9. Symbol error rate (SER) performance versus signal to noise ratio (SNR), for 4-PSK and 4-QAM modulation of the source symbols, the sub-optimal detection method for superposition coded cooperation (SCC) and superposition network coded cooperation (SNCC), $c_1 = 0.99$, $\lambda_1 = 0.5$, $\lambda_2 = 0.4$, $\lambda_3 = 0.3$, $\lambda_4 = 0.2$, and $\lambda_5 = 0.1$.

7. CONCLUSION

In this paper, we proposed a new TDMA-based cooperative scheme for wireless networks to achieve better communication performance than the non-cooperative and the SCC scheme. This was obtained by using a combination of superposition coding and network coding. The scheme was named SNCC and was described in detail for the general case. It was seen from analytical and simulation results that in comparison with non-cooperative communication, SNCC improves the performance of the first $n - 1$ users significantly, while it degrades the performance of the last user. Although by choosing c_1 sufficiently close to 1 the performance degradation of the last user can be made to be arbitrarily small, it weakens the cooperative advantages of SNCC for other users. So the coefficient c_1 needs to be chosen in an efficient manner to gain an acceptable performance improvement for the first $n - 1$ users without significant degradation in the performance of the last user. It was also seen that the performance of SNCC is always better than SCC. These advantages are provided by SNCC without any additional time slot requirements compared with SCC and TDMA-based non-cooperative schemes.

APPENDIX A: DERIVATION OF (10)

We show that if condition (10) is satisfied, then the II detector has the same performance as the optimal ML detector in detecting the source symbol s_i from $y_{i,j}$. From (6), the decision region of the k th constellation point of s_i when II detector is used is equal to

$$r_k = \left\{ r : \left| r - h_{i,j} c_{1,i} a e^{j \frac{2\pi}{M} k} \right| < \left| r - h_{i,j} c_{1,i} a e^{j \frac{2\pi}{M} z} \right|, \forall z \neq k \right\} \quad (54)$$

If (10) is satisfied, the term $\psi_{k,m}$ in (8) can be written as $\psi_{k,m} = \frac{c_{1,i}}{\beta_m} a e^{j \frac{2\pi}{M} k}$, where $\beta_m > 0$. Therefore, we can write (54) using $\psi_{k,m}$ as

$$r_k = \left\{ r : |r - \beta_m h_{i,j} \psi_{k,m}| < |r - \beta_m h_{i,j} \psi_{z,m}|, \beta_m > 0, \forall z \neq k, \forall m \right\} \quad (55)$$

From (8), $\psi_{k,m}$ and $\psi_{z,m}$ are signal points of a M-PSK constellation. Because multiplying points of a M-PSK constellation by a positive number β_m does not change decision regions for that constellation, (55) can be written as

$$r_k = \left\{ r : |r - h_{i,j} \psi_{k,m}| < |r - h_{i,j} \psi_{z,m}|, \forall z \neq k, \forall m \right\} \quad (56)$$

Finally, because the function e^{-x} is monotonically decreasing, (56) may be rewritten as

$$r_k = \left\{ r : \sum_m e^{-\frac{|r - h_{i,j} \psi_{k,m}|^2}{N_0}} > \sum_m e^{-\frac{|r - h_{i,j} \psi_{z,m}|^2}{N_0}}, \forall z \neq k \right\} \quad (57)$$

However, r_k is the decision region of the optimal ML detector corresponding to the k th constellation point of s_i [29]. Therefore, the decision regions of the II detector are the same as the optimal ML detector. This means that the II detector has the same performance as the optimal ML detector.

APPENDIX B: SUBOPTIMAL DETECTION PROCEDURE

It can be easily verified that the suboptimal detection procedure satisfies Conditions I and II for $n = 2$. Now, we assume that the procedure satisfies Conditions I and II for $n = k, k > 2$ and use induction for $n = k + 1$. The following definition and simple lemmas are used for the proof.

Definition. For arbitrary real numbers r_1, r_2, r_3, r_4 , two unordered pairs $\{r_1, r_2\}$ and $\{r_3, r_4\}$ are equal if $r_1 = r_3$ and $r_2 = r_4$ or $r_1 = r_4$ and $r_2 = r_3$.

Lemma 1. For arbitrary real numbers r_1, r_2 , and r_3 , the unordered pairs $\omega_1 = \{\text{Max}\{r_1, r_2\}, r_3\}$ and $\omega_2 = \{\text{Max}\{r_1, r_2, r_3\}, \text{Min}\{\text{Max}\{r_1, r_2\}, r_3\}\}$ are equal, so they are exchangeable. In other words, these sets can be exchanged in the process of detection.

Lemma 2. For arbitrary real numbers r_1, r_2 and r_3 , the pairs $\omega_3 = \{\text{Max}\{r_1, r_2\}, \text{Max}\{r_3, \text{Min}\{r_1, r_2\}\}\}$ and $\omega_4 = \{\text{Max}\{r_1, r_2, r_3\}, \text{Med}\{r_1, r_2, r_3\}\}$ are equal. Thus, $\omega_5 = \{\text{Max}\{r_1, r_3\}, \text{Max}\{r_2, \text{Min}\{r_1, r_3\}\}\}$ is also equal to ω_4 , and hence, equal to ω_3 .

Lemma 3. For real numbers r_1, r_2 and r_3 with $r_1 > r_3$, $\text{Min}\{r_1, \text{Max}\{r_2, r_3\}\} = \text{Med}\{r_1, r_2, r_3\}$.

Expanding the detection procedure, for $n = k, k > 2$, results in

$$\begin{aligned} M_1 &= \text{Max}\{P_{cs1}, P_{cs2}\}, \\ M_2 &= \text{Max}\{\Omega_2, P_{cs3}\}, \\ &\vdots \\ M_{k-2} &= \text{Max}\{\Omega_{k-2}, P_{cs_{k-1}}\}, \\ M_{k-1} &= \text{Max}\{\Omega_{k-1}, P_{cs1, \dots, k-1}\}, \\ Q_k &= \{\text{Sym}\{M_1\}, \dots, \text{Sym}\{M_{k-1}\}, s_k \} \end{aligned} \quad (58)$$

where Q_k includes the best symbols from the set $\Psi_k = \{s_1, s_2, \dots, s_k, s_{1,1}, \dots, s_{1, \dots, k-1}\}$ to detect $\phi_k = \{s_1, \dots, s_k\}$ and

$$\Omega_i = \underbrace{\text{Med}\{\dots \text{Med}\{P_{cs1}, P_{cs2}, P_{cs1,1}\}, \dots\}}_{i-1}, P_{cs_i}, P_{cs1, \dots, i-1} \} \quad (59)$$

For $n = k + 1$, the receiver must choose the best symbols from Ψ_{k+1} to detect the symbols in ϕ_{k+1} . The set Ψ_{k+1} is $\Psi_k \cup \{s_{k+1}, s_{1, \dots, k}\}$. The symbol s_{k+1} is the only symbol in Ψ_{k+1} bearing the information of s_{k+1} .

Hence, it is the unique choice from Ψ_{k+1} to detect s_{k+1} , which means that its selection is necessary. Hence, the problem is simplified to selecting the best k symbols from the set $\Psi'_k = \Psi_k \cup \{s_{1,\dots,k}\}$ to obtain the symbols in ϕ_k . This problem can be solved by dividing it in two parts:

- I- If the symbol s_k is selected from Ψ'_k , the symbols $s_{1,\dots,k-1}$ and $s_{1,\dots,k}$ are exchangeable in the selection process, because using $s_k, s_{1,\dots,k-1} \oplus s_k = s_{1,\dots,k}$. Thus, selecting the best k symbols from Ψ'_k is equivalent to selecting the best k symbols from Ψ_k , according to (58), by replacing $P_{CS_{1,\dots,k-1}}$ with $\text{Max}\{P_{CS_{1,\dots,k-1}}, P_{CS_{1,\dots,k}}\}$. In summary, if symbol s_k is selected, the detection procedure can be written as

$$\begin{aligned} M_{1,1} &= \text{Max}\{P_{CS_1}, P_{CS_2}\}, \\ M_{2,1} &= \text{Max}\{\Omega_2, P_{CS_3}\}, \\ &\vdots \\ M_{k-2,1} &= \text{Max}\{\Omega_{k-2}, P_{CS_{k-1}}\}, \\ M_{k-1,1} &= \text{Max}\{\Omega_{k-1}, P_{CS_{1,\dots,k-1}}, P_{CS_{1,\dots,k}}\}, \\ M_{k,1} &= P_{CS_k}, \\ \varrho_{k+1}^1 &= \{\text{Sym}\{M_{1,1}\}, \dots, \text{Sym}\{M_{k,1}\}, s_{k+1}\} \end{aligned} \quad (60)$$

$$\varrho_{k+1} = \{\text{Sym}\{M_{1,1}\}, \text{Sym}\{M_{2,1}\}, \dots, \text{Sym}\{M_{k-1,1}\}, \text{Sym}\{M'_k\}, s_{k+1}\} \quad (64)$$

- II- If symbol s_k is not selected from Ψ'_k , the symbol $s_{1,\dots,k}$ must inevitably be chosen, because it is the only symbol that contains the information of s_k . In this case the receiver must select the best $k-1$ symbols from the set $\Psi''_k = \Psi_{k-1} \cup \{s_{1,\dots,k-1}\}$ to obtain the symbols in ϕ_{k-1} . From (58), it is apparent that $\text{Sym}\{M_1\}, \dots, \text{Sym}\{M_{k-1}\}$ are these symbols. Consequently, in this case, the best $k+1$ symbols are determined according to following procedure

$$\begin{aligned} M_{1,2} &= \text{Max}\{P_{CS_1}, P_{CS_2}\}, \\ M_{2,2} &= \text{Max}\{\Omega_2, P_{CS_3}\}, \\ &\vdots \\ M_{k-2,2} &= \text{Max}\{\Omega_{k-2}, P_{CS_{k-1}}\}, \\ M_{k-1,2} &= \text{Max}\{\Omega_{k-1}, P_{CS_{1,\dots,k-1}}\}, \\ M_{k,2} &= P_{CS_{1,\dots,k}}, \\ \varrho_{k+1}^2 &= \{\text{Sym}\{M_{1,2}\}, \dots, \text{Sym}\{M_{k,2}\}, s_{k+1}\} \end{aligned} \quad (61)$$

According to Lemma 1, $o_1 = \{M_{k-1,2}, M_{k,2}\}$ is equal to $o_2 = \{M'_{k-1,2}, M'_{k,2}\}$ where

$$\varrho_{k+1} = \{\text{Sym}\{M_{1,1}\}, \text{Sym}\{M_{2,1}\}, \dots, \text{Sym}\{M'_{k-1}\}, \text{Sym}\{M'_k\}, s_{k+1}\} \quad (68)$$

$$\begin{aligned} M'_{k-1,2} &= \text{Max}\{\Omega_{k-1}, P_{CS_{1,\dots,k-1}}, P_{CS_{1,\dots,k}}\} \text{ and} \\ M'_{k,2} &= \text{Min}\{\text{Max}\{\Omega_{k-1}, P_{CS_{1,\dots,k-1}}\}, P_{CS_{1,\dots,k}}\} \end{aligned} \quad (62)$$

So the terms in (62) can be replaced with $M_{k-1,2}$ and $M_{k,2}$ in (61). In other words, the detection procedure in (61) can be written in another form as

$$\begin{aligned} M_{1,2} &= \text{Max}\{P_{CS_1}, P_{CS_2}\}, \\ M_{2,2} &= \text{Max}\{\Omega_2, P_{CS_3}\}, \\ &\vdots \\ M_{k-2,2} &= \text{Max}\{\Omega_{k-2}, P_{CS_{k-1}}\}, \\ M'_{k-1,2} &= \text{Max}\{\Omega_{k-1}, P_{CS_{1,\dots,k-1}}, P_{CS_{1,\dots,k}}\}, \\ M'_{k,2} &= \text{Min}\{\text{Max}\{\Omega_{k-1}, P_{CS_{1,\dots,k-1}}\}, P_{CS_{1,\dots,k}}\}, \\ \varrho_{k+1}^2 &= \{\text{Sym}\{M_{1,2}\}, \dots, \text{Sym}\{M'_{k-1,2}\}, \text{Sym}\{M'_{k,2}\}, s_{k+1}\} \end{aligned} \quad (63)$$

The receiver selects one of the sets ϱ_{k+1}^1 or ϱ_{k+1}^2 given in (60) and (63), respectively, to achieve the best path of detecting the required symbols. Now, we must determine how the receiver selects the best of these two sets. By comparing (60) with (63), it can be seen that all elements in the sets ϱ_{k+1}^1 and ϱ_{k+1}^2 are the same except for $M_{k,1}$ and $M'_{k,2}$. Therefore, the best path for the receiver is

where

$$M'_k = \text{Max}\{\text{Min}\{\text{Max}\{\Omega_{k-1}, P_{CS_{1,\dots,k-1}}\}, P_{CS_{1,\dots,k}}\}, P_{CS_k}\} \quad (65)$$

By setting $r_1 = \text{Max}\{\Omega_{k-1}, P_{CS_{1,\dots,k-1}}\}$, $r_2 = P_{CS_{1,\dots,k}}$ and $r_3 = P_{CS_k}$, the set $o_3 = \{M_{k-1,1}, M'_k\}$ has the same form as ω_3 in Lemma 2. From the equality of ω_3 and ω_5 in Lemma 2, o_3 is equal to $o_5 = \{M'_{k-1}, M''_k\}$ where

$$\begin{aligned} M'_{k-1} &= \text{Max}\{\Omega_{k-1}, P_{CS_k}, P_{CS_{1,\dots,k-1}}\} \text{ and} \\ M''_k &= \text{Max}\{\text{Min}\{P_{CS_k}, \text{Max}\{\Omega_{k-1}, P_{CS_{1,\dots,k-1}}\}\}, P_{CS_{1,\dots,k}}\} \end{aligned} \quad (66)$$

Finally, because for an arbitrary user i , the greater portion of power is allocated to the source symbol s_i , $P_{CS_i} > P_{CS_{1,\dots,i-1}}$. Thus, by applying Lemma 3

$$M''_k = \text{Max}\{\text{Med}\{\Omega_{k-1}, P_{CS_k}, P_{CS_{1,\dots,k-1}}\}, P_{CS_{1,\dots,k}}\} \quad (67)$$

Because of the equality of o_3 and o_5 , the best path for detection, given in (64), can be written as

which are the points resulting from the detection procedure in Section 3.2, for $n = k + 1$. This proves that Conditions I and II are satisfied when using the sub-optimal procedure of Section 3.2.

APPENDIX C: LOWER BOUNDS FOR $P_{cs_k}, P_{cs_1, \dots, l}$

This appendix demonstrates how the lower bounds in (29) are achieved. We only derive the bounds for M-PSK modulation. By following a similar approach, the results for M-QAM modulation are straightforward. Consider the detection process of the source symbol s_i from y_i in (5) using the II detector. According to (8) for a M-PSK modulation of the source symbols, there are M^2 equiprobable constellation points for transmitted symbol s_i . So the probability of correct detection of s_i may be written as

$$P_{cs_i} = 1 - \frac{1}{M^2} \sum_{k=1}^M \sum_{m=1}^M P_{e|\psi_{k,m}} \quad (69)$$

where $P_{e|\psi_{k,m}}$ is the probability of error in detecting symbol s_i , if the signal point $\psi_{k,m}$, given in (8), is transmitted. According to (8), the constellation points of x_i are symmetric, so $P_{e|\psi_{k,m}} = P_{e|\psi_{M,m}}$ for all k . Therefore, (69) can be simplified to

$$P_{cs_i} = 1 - \frac{1}{M} \sum_{m=1}^M P_{e|\psi_{M,m}} \quad (70)$$

Now suppose that the transmitted symbol is $\psi_{M,m}$. From (6), assuming that (10) is satisfied, the decision region of the II detector for correct detection of the symbol s_i from the received signal y_i , is $h_i r e^{j\theta}$, $r > 0$, $-\frac{\pi}{M} < \theta < \frac{\pi}{M}$. Therefore, the symbol $h_i \psi_{M,m}$ is surrounded by $N_s = 2$ decision boundaries with minimum distance $d_{\min} = |h_i| \sin(\frac{\pi}{M}) \psi_{M,m}$. According to (3) and (8), d_{\min} can be written as

$$d_{\min} = \begin{cases} a|h_1| \sin(\frac{\pi}{M}), & i = 1; \\ a|h_i|u_m, & i \neq 1 \end{cases} \quad (71)$$

where $u_m = \left(c_1 + A_m \sqrt{\frac{3(1-c_1^2)}{M^2-1}} \right) \sin(\frac{\pi}{M})$. By the use of the nearest neighbour union bound (NNUB) approximation [33], a good upper bound for $P_{e|\psi_{M,m}}$ is

$$P_{e|\psi_{M,m}} < N_s Q \left(\frac{d_{\min}}{\sqrt{\frac{N_0}{2}}} \right) \quad (72)$$

By substituting (71) in (72) and then (72) in (70), the lower bound for P_{cs_i} , $i > 1$ is obtained as

$$P_{cs_i} > 1 - \frac{2}{M} \sum_{m=1}^M Q \left(u_m \sqrt{2|h_i|^2 \text{SNR}} \right) \quad (73)$$

where, $\text{SNR} = \frac{a^2}{N_0}$. Also, for $i = 1$, P_{cs_i} can be approximated as

$$\begin{aligned} P_{cs_1} &> 1 - 2Q \left(\sin(\frac{\pi}{M}) \sqrt{2|h_1|^2 \text{SNR}} \right) \\ &> 1 - 2Q \left(\frac{1}{M} \sum_{m=1}^M u_m \sqrt{2|h_i|^2 \text{SNR}} \right) \\ &> 1 - \frac{2}{M} \sum_{m=1}^M Q \left(u_m \sqrt{2|h_i|^2 \text{SNR}} \right) \end{aligned} \quad (74)$$

where the first inequality can be obtained by the NNUB approximation. Also, because $\frac{1}{M} \sum_{m=1}^M u_m = c_1 \sin(\frac{\pi}{M})$, $c_1 < 1$, the second inequality can be verified. Finally, as the Q-function is convex, the third inequality in (74) is obtained. From (74) it can be concluded that the lower bound in (73) is valid for $i \geq 1$.

By using the NNUB approximation and following the same approach as (74), a lower bound for $P_{cs_1, \dots, l}$ can be obtained as

$$\begin{aligned} P_{cs_1, \dots, l} &> 1 - 2Q \left(v' \sqrt{2|h_{l+1}|^2 \text{SNR}} \right) \\ &> 1 - 2Q \left(\frac{1}{M} \sum_{m=1}^M \frac{u_m}{\sin(\frac{\pi}{M})} \cdot v' \sqrt{2|h_{l+1}|^2 \text{SNR}} \right) \\ &> 1 - \frac{2}{M} \sum_{m=1}^M Q \left(\frac{u_m}{\sin(\frac{\pi}{M})} \cdot v' \sqrt{2|h_{l+1}|^2 \text{SNR}} \right) \end{aligned} \quad (75)$$

where $v' = \sqrt{\frac{3(1-c_1^2)}{M^2-1}}$.

REFERENCES

1. Tse D, Viswanath P. *Fundamentals of Wireless Communication*. Cambridge University Press: New York, 2005.
2. Sendonaris A, Erkip E, Aazhang B. User cooperation diversity Part I: system description. *IEEE Transactions on Communications* 2003; **51**(11): 1927–1938.
3. Sendonaris A, Erkip E, Aazhang B. User cooperation diversity Part II: implementation aspects and performance analysis. *IEEE Transactions on Communications* 2003; **51**(11): 1939–1948.
4. Rodrigo P. *Resource Allocation and MIMO for 4G and Beyond*. Springer: New York, 2014.
5. Elgendi M, Nasr OA, Khairy MM. Cooperative multicasting based on superposition and layered coding. *IET Communications* 2014; **8**(3): 267–277.
6. Uysal M. *Cooperative Communications For Improved Wireless Network Transmission Framework for Virtual Antenna Array Applications*. Information Science Reference: New York, 2009.
7. Laneman JN, Tse D, Wornell GW. Cooperative diversity in wireless networks: efficient protocols and outage behavior. *IEEE Transactions on Information Theory* 2004; **50**(12): 3062–3080.

8. Sadek AK, Su W, Liu KJR. Multinode cooperative communications in wireless networks. *IEEE Transactions on Signal Processing* 2007; **5**(1): 341–355.
9. Ribeiro A, Cai X, Giannakis GB. Symbol error probabilities for general cooperative links. *IEEE Transactions on Wireless Communications* 2005; **4**(3): 1264–1273.
10. Anghel PA, Kaveh M. Exact symbol error probability of a cooperative network in a Rayleigh-fading environment. *IEEE Transactions on Wireless Communications* 2004; **3**(5): 1416–1421.
11. Laneman JN, Wornell GW. Distributed space-time coded protocols for exploiting cooperative diversity in wireless networks. *IEEE Transactions on Information Theory* 2003; **49**(10): 2415–2425.
12. Jing Y, Hassibi B. Distributed space-time coding in wireless relay networks. *IEEE Transactions on Wireless Communications* 2006; **5**(12): 3524–3536.
13. Venturino L, Wang X, Lops M. Multiuser detection for cooperative networks and performance analysis. *IEEE Transactions on Signal Processing* 2006; **54**(9): 3315–3329.
14. Seddik KG, Sadek AK, Su W, Liu KJR. Outage analysis and optimal power allocation for multinode relay networks. *IEEE Signal Processing Letter* 2007; **14**(6): 377–380.
15. Jagannathan S, Aghajan H, Goldsmith A. The effect of time synchronization errors on the performance of cooperative MISO systems. In *Proceedings of IEEE GlobeCom*, Dallas, Texas, USA, 2004; 102–107.
16. Li X, Wu YC, Serpedin E. Timing synchronization in decode-and-forward cooperative communication systems. *IEEE Transactions on Signal Processing* 2009; **57**(4): 1444–1455.
17. Dai M, Sung CW. Achieving high diversity and multiplexing gains in the asynchronous parallel relay network. *Transactions on Emerging Telecommunications Technologies* 2013; **24**(2): 232–243.
18. Lai HQ, Liu KJR. Space-time network coding. *IEEE Transactions on Signal Processing* 2011; **59**(4): 1706–1718.
19. Lai HQ, Ibrahim AS, Liu KJR. Wireless network cocast: location-aware cooperative communications with linear network coding. *IEEE Transactions on Wireless Communications* 2009; **8**(7): 3866–3854.
20. Larsson EG, Vojcic BR. Cooperative transmit diversity based on superposition modulation. *IEEE Communication Letters* 2005; **9**(9): 778–780.
21. Dai M, Wang H, Lin X, Zhang S, Chen B. Opportunistic relaying with analogue and digital network coding for two-way parallel relay network. *IET Communications* 2014; **8**(12): 2200–2206.
22. Shi S, Yang L, Zhu H. A novel cooperative transmission scheme based on superposition coding and partial relaying. *International Journal of Communication Systems* 2014; **27**: 2889–2908.
23. Meng Y, Liu G, Shen G, Liu Z, Jiang Q, Tang Y. Superposition coding and analysis for cooperative multiple access relay system. *Wireless Personal Communication* 2013; **70**: 1011–1028.
24. Zhang B, Hu J, Huang Y, El-Hajjar M, Hanzo L. Outage analysis of superposition-modulation-aided network-coded cooperation in the presence of network coding noise. *IEEE Transactions on Vehicular Technology* 2015; **64**(2): 493–501.
25. Vanka S, Srinivasa S, Gong Z, Vizi P, Stamatiou K, Haenggi M. Superposition coding strategies: design and experimental evaluation. *IEEE Transactions on Wireless Communications* 2012; **11**(7): 2628–2639.
26. Librino F, Zorzi M. Performance of advanced decoding schemes for uplink relaying in cellular networks. *IEEE Transactions on Communications* 2015; **63**(1): 79–93.
27. Ahlswede R, Cai N, Li SYR, Yeung RW. Network information flow. *IEEE Transactions on Information Theory* 2000; **46**(4): 1204–1216.
28. Hammerstrom I, Kuhn M, Esli C, Zhao J, Wittneben A, Bauch G. MIMO two-way relaying with transmit CSI at the relay. In *Proceedings of the IEEE Workshop on Signal Processing Advances in Wireless Communications*, Helsinki, Finland, June 2007; 1–5.
29. Lee J, Toumpakaris D, Yu W. Interference mitigation via joint detection in a fading environment. In *Information Theory and Applications Workshop (ITA)*, La Jolla, California, February 2011; 1–7.
30. Proakis JG, Salehi M. *Digital Communications* (5th edn). McGraw-Hill: New York, 2008.
31. Cui S, Goldsmith A, Bahai A. Energy-constrained modulation optimization. *IEEE Transactions on Wireless Communications* 2005; **4**(5): 2349–2360.
32. Sediq AB, Yanikomeroglu H. Performance analysis of selection combining of signals with different modulation levels in cooperative communications. *IEEE Transactions on Vehicular Technology* 2011; **60**(4): 1880–1887.
33. Goldsmith A. *Wireless Communications*. Cambridge Univ. Press: New York, 2005.